Chapter 7

Methodology for the Low-Cost Optimisation of Small-Wind Turbines

Alberto Arroyo, Mario Manana, Pablo B. Castro,
Raquel Martinez, Ramon Lecuna and Juan Carcedo

Additional information is available at the end of the chapter

http://dx.doi.org/10.5772/63432

Abstract

The increasing use of small-wind energy has made it necessary to develop new methods that improve the efficiency of this technology. This is best done by considering the interaction between the various components, such as wind rotors, electrical generators, rectifiers and inverters, as opposed to studying the individual components in isolation.

Hence, this chapter describes a methodology to increase the efficiency of small-wind turbines (SWTs) equipped with an electrical machine, rectifier and inverter. To achieve this objective, capacitor banks will be connected between the electrical machine and the rectifier.

This methodology is motivated by two clear aims. The first one is to operate the SWT with its maximum power coefficient (C_p). The second one is to select the most suitable capacitor bank for each wind speed in order to optimise the energy supplied to the grid.

Keywords: capacitor, wind power generation, performance optimisation, Weibull distribution, renewable energy

1. Introduction

The fact that everyday more wind power is used demands the development of new technologies of electronic production and the improvement of existing ones. The humankind challenge will be, on the one hand, trying to satisfy the demands of the aforementioned energy and on the other, being respectful to the environment in order to stop the climate change that is taking place.

Thus, wind power is one of the energies that have been developed in order to satisfy this demand and be respectful to the environment. Recently, this energy has become one of the main sustainable sources used in developing countries.

The wind can generate electric power without producing undesirable pollutants associated with fossil fuels and nuclear energy. In addition, wind power is a potentially unlimited resource unlike fossil fuels and the elements used in nuclear power plants. Furthermore, wind power promotes a clear and sustainable energy future without the use of fossil fuel resources.

The wind industry promotes a clean and sustainable energy future distinct from the fossil resources. It is for this reason that the wind sector is the one which has experienced the biggest growth in recent years.

Historically, wind power was linked to windmills on land. However, nowadays, this trend is changing due to the discovery of the big benefits that these windmills would produce on the coast. Some of the main advantages of the off-shore farms are large usable wind power, the reduction of the visual impact and the reduction of mortality levels of birds.

Therefore, wind power is not new but one of the oldest energies together with the thermal energies. The wind, as a driving force is, was already used in olden days, for instance, to move the millstones that grind the wheat to produce flour. In the same way, ships were moved driven by the wind.

However, in the early 1980s, this type of renewable energy began to develop and is still being used. Since the year 2000, the wind power industry has been spreading all over the world, especially in Germany, the USA, Denmark and Spain. It is not necessary to go deeply into the issue but the main factor that produces such a development is the good wind condition found in those countries.

As mentioned earlier, the development of the modern turbines began from the 80s decade. Since then, the wind power sector has undergone a vertiginous increase; thus, nowadays, wind power has become one of the main supports of the worldwide economy.

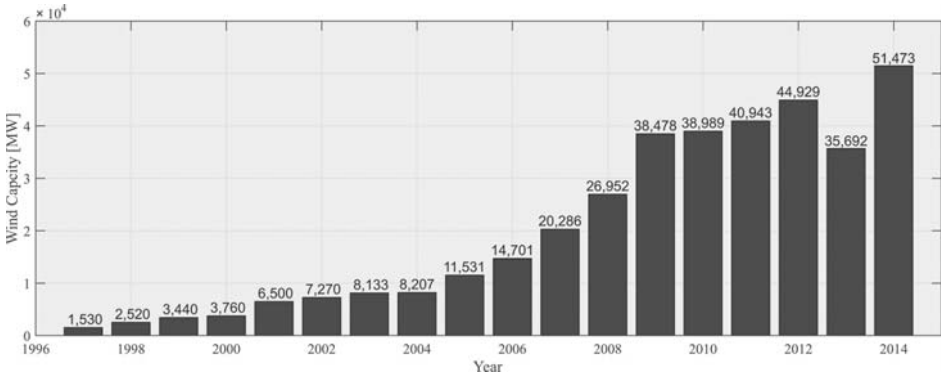

Figure 1. Global annual installed wind capacity 1997–2014. Adapted from reference [1].

http://dx.doi.org/10.5772/63432

According to the Global Wind Report created by the Global Wind Energy Council (GWEC), from 1996, the development of the world wind power has undergone a substantial increase. In 2010, this development was slowed down because of the crisis.

In **Figure 1**, variation of the global annual installed wind capacity in MW can be observed. In the aforementioned figure, it can be also observed how the crisis, as in all sectors, slowed down the development of the world installed power.

In **Figure 2**, the increase in the wind power that was produced worldwide, for several regions, can be perceived. It is important to take into account that the wind capacity development was different depending on the continent. It seems logical that in underdeveloped countries, there is a lower economic capacity to install this energy. Nevertheless, in 2014, a new increase in the wind capacity was produced.

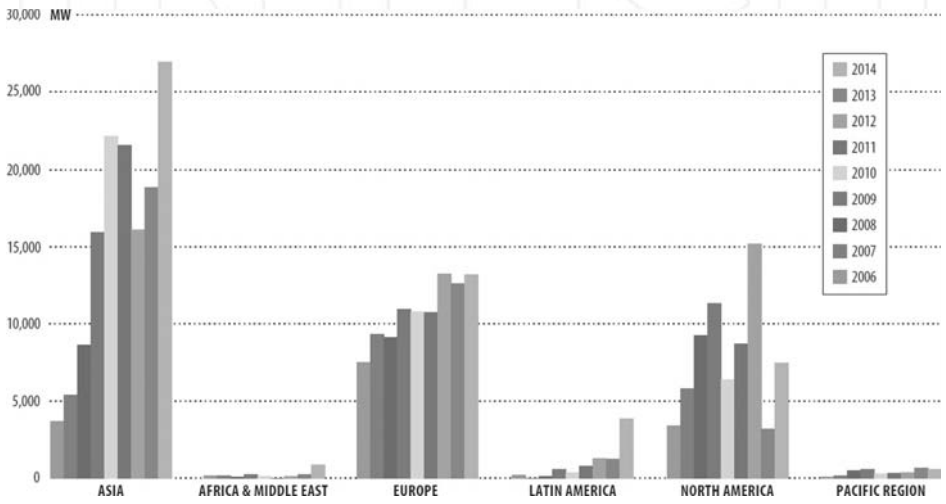

Figure 2. Annual installed wind capacity by region 2006–2014. Adapted from reference [1].

In the aforementioned figure, various details can be observed:

- First, the current power installed in Europe and North America was gradually increased until 2010, when it experienced the crisis.
- Second, the crisis has not influenced the wind power sector in Asia where the production even increased in 2010.
- Third, the installed power in Europe, Asia and North America is substantially higher than in other regions such as Latin America, Africa, the Middle East and the Pacific.
- Finally, it can be observed that in Latin America, Africa, Middle East and Pacific, production begins to increase gradually.

Although it is foreseen that the conventional installed wind power will continue to increase, sooner or later this growth will stop. Due to the fact that this moment is close in certain countries, the study, development and implementation of the small-wind energy will be a good point to continue working.

Although small-wind turbines (SWTs) do not supply as much power as bigger ones, their implementation has a wide range of possibilities because they can be located in other places such as roofs. In addition, they can work in isolated power systems and supply without any other means of alternative energy when the average wind speed allows it.

Of course, this option does not imply the total retirement of other types of energies such as the nuclear or thermal ones. However, this may imply the reduction in the amount of thermal and nuclear power stations in those places. In this way, each citizen may self-supply part of his daily energy. If a whole country is considered, the produced energy will be substantially reduced as well as the harmful effects on the environment. Both wind powers have been exhaustively studied, giving different kinds of settings.

The USA is the country with the largest development of the small-wind industry. In 2009, the USA had an installed wind capacity of 100 MW, and it has a prevision of exponential growth in the upcoming years. In the same continent, Canada has the aim of reaching 60 MW capacity.

In Europe, the country that has developed this energy the most is the UK due to the implementation of several strategies. These strategies establish that by 2050, 30–40% of the energy demand will be covered by microgeneration technologies.

In France and Italy, there is a trend for this type of energy with plans and decrees that enact the installation of small-wind power. Portugal strongly promotes this industry with the Decree 362/2oo7, where subsidies and bonuses for the small-wind energy producers are established. This makes a total difference with the traditional wind energy, unlike countries such as Spain.

In Spain, small-wind energy, despite its numerous advantages, is not developed enough due to legislative, economic, technological and social barriers. Despite its low development, the people in charge of this industry state that this renewable energy has great potential.

The key to increase the production and to decrease the costs is the development of new materials and new manufacturing techniques.

2. Description of the methodology

2.1. Introduction

This chapter presents a methodology to optimise the efficiency of SWTs. To test this methodology, it is necessary to create a model of the whole system. To optimise the system, two aspects are considered:

- The aerodynamic factor: The maximum power point tracker (MPPT) [2] is calculated to extract the maximum energy from the wind [3]. Using the MPPT and the SWT operating

http://dx.doi.org/10.5772/63432

surfaces, the optimal relationship between the continuous voltage of the rectifier and the grid power can be determined. This relationship must be set in the inverter, and it is known as the maximum power characteristic curve (MPCC).

- The capacitor bank effect: When a capacitor bank is connected, the armature reaction produces a magnetising effect in the electrical machine that is added to the magnetic field generated by the magnets. Therefore, a higher voltage at the machine terminals is generated [4, 5]. Then, before connecting a capacitor bank, some subjects have to be analysed. It must be verified that

○ The current increment, which produces the capacitor bank, does not damage the electrical machine windings. It should be noticed that if this methodology is used in a commercial SWT, the winding wire diameter cannot be changed. Thus, this current increment must be limited.

○ The magnetic saturation increment, which produces the capacitor bank, does not increase the iron losses too much.

2.2. Obtain the MPPT of an SWT

To be able to understand the calculation of MPCCs, you should first understand how the SWT operates. Thus, you will study the maximum power that can be extracted from the wind kinetic energy and the main characteristic parameters of the SWTs.

To perform this study, it is necessary to start from the beginning, the wind. As it is known, the wind is made up of particles in motion. In this way, when these particles find in their path an element (SWT blades) that can rotate about a shaft (either horizontal or vertical), they make it rotate. And if this shaft has got an electrical machine, the electricity is generated.

The air mass before passing through the SWT has got a kinetic energy. This kinetic energy can be expressed according to Eq. (1).

$$E_c = \frac{1}{2} m u^2 \tag{1}$$

where E_c is the air kinetic energy (J), m is the air mass (kg) and u is the air velocity (m/s).

The wind, in its path through SWT blades, suffers a decrease in its speed or what is the same a decrease in its kinetic energy. This lost kinetic energy is transformed, by means of the SWT blades, into mechanical energy. And the electrical generator transforms this mechanical energy into electrical energy [6].

To follow, a study of the air performance, when it passes through the SWT, will be made. This study led us to obtain an expression to calculate the maximum mechanical power that can be extracted from the wind. For this analysis, an air stream tube will be considered (**Figure 3**). This tube is formed by air lines in the laminar regime, parallel to the wind and with an axial symmetry.

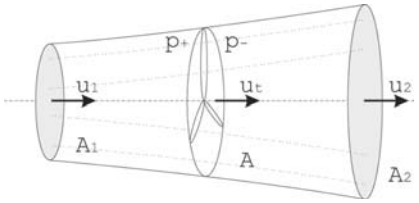

Figure 3. Airflow before and after wind turbine.

In the stream tube, the following parameters can be seen: air velocity at inlet of tube u_1 (m/s), air velocity at outlet of tube u_2 (m/s), air velocity in turbine u_h (m/s), air pressure before the turbine p_+ (Pa), air pressure after the turbine p_- (Pa), area at inlet of tube A_1 (m^2), area at outlet of tube A_2 (m^2) and area of the tube in turbine A (m^2).

Let us consider the mechanical power P_w extracted from wind as the loss of air kinetic energy due to its passage through the SWT, then the following equation can be obtained:

$$P_w = \Delta\varepsilon_c = \varepsilon_{c1} - \varepsilon_{c2} = \frac{1}{2}mu_1^2 - \frac{1}{2}mu_2^2 = \rho u_h \frac{\pi d^2}{4}\left(\frac{1}{2}u_1^2 - \frac{1}{2}u_2^2\right) \tag{2}$$

where E_{c1} is the kinetic energy at inlet of tube (J), E_{c2} is the kinetic energy at outlet of tube (J), ρ is the air density (kg/m^3) and d is the diameter of turbine blades (m).

Studying the Froude's theorem [6], it can be understood that the air average velocity in its passage through the stream tube is the arithmetic mean of u_1 and u_2. Thus:

$$u_h = \frac{u_1 + u_2}{2} \tag{3}$$

Eq. (3) can also be obtained as follows:

- The air velocity at inlet of tube u_1.
- The air velocity, as it approaches the turbine, is modified. In this way, its value will be u_1 minus an axial-induced velocity, which is known as u_a (**Figure 3**).

Consequently, it can be established that:

$$u_a = au_1 \tag{4}$$

$$u_h = u_1 - u_a \tag{5}$$

Or what is the same:

http://dx.doi.org/10.5772/63432

$$u_h = u_1(1-a) \tag{6}$$

Thus, the velocity u_2 will be:

$$u_2 = u_1(1-2a) \tag{7}$$

where a is the induced axial velocity coefficient, which is opposed to velocity u_1.

Thus, Eq. (2), (6) and (7) yield the following relation:

$$P_w = \frac{1}{2}\frac{\pi d^2}{4}\rho u_1^3(1-a)(1-(1-2a)^2) \tag{8}$$

The next step will be to derive Eq. (8) with respect to a and make it equal to zero. Then, the value of a, for which P_w is maximised, will be obtained.

$$\frac{\partial P_w}{\partial a} \rightarrow a = \frac{1}{3} \tag{9}$$

Thus, if a = 1/3 is replaced with Eq. (8), the following equation is obtained:

$$P_{w,max} = \frac{16}{27}\left(\frac{1}{2}\frac{\pi d^2}{4}\rho u_1^3\right) \tag{10}$$

Eq. (10) is usually expressed in a dimensionless way as the power coefficient (C_p):

$$C_p = \frac{P_w}{\frac{1}{2}\cdot\frac{\pi d^2}{4}\rho u_1^3} \tag{11}$$

Thus, C_p represents the percentage of power extracted from the wind kinetic energy. The maximum value that C_p might take is 16/27 = 0.593. This value is called *Betz limit* [7] and provides the maximum mechanical power P_w that can be extracted from wind kinetic energy, regardless of SWT type. In summary, no SWT will be able to extract more wind power than the *Betz limit* states.

The *Betz limit* is an upper limit. However, it does not mean that all SWTs can extract that upper limit. In fact, the *Betz limit* does not take into account several parameters that reduce this upper limit. Some of these parameters are aerodynamic roughness of blades due to their ageing, lost energy due to wake generated by the rotation, air properties, interference of blades, direction of SWT (ψ), pitch angle (β) and SWT shape.

In this way, C_p will be a function of the SWT diameter, wind speed, air density, air viscosity, blade roughness, SWT shape, SWT rotation speed and SWT angles.

Of all these parameters, the viscosity and the roughness can be initially ignored due to their small influence on the final results. The SWT orientation can be also ignored because the SWT is usually orientated in the wind direction. Furthermore, if you have a SWT-specific shape, it can also be assumed that C_p does not depend on it.

Thus, it is concluded that for this study C_p will be function of diameter d, wind speed u_h, SWT rotation speed ω and pitch angle β.

$$C_p = f(d, u_h, \omega, \beta) \tag{12}$$

Taking all this into account, it seems logical to think in a coefficient that includes all these parameters. This coefficient is the tip-speed ratio λ, and it is defined as:

$$\lambda = \frac{Speedo\ frotortip}{Windspeed} = \frac{\frac{\omega d}{2}}{u_h} \tag{13}$$

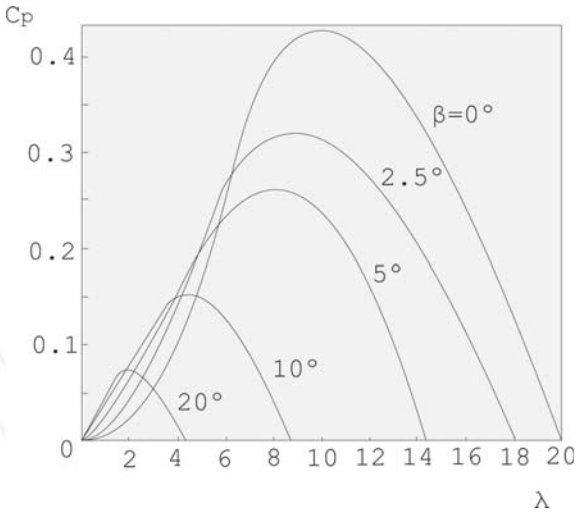

Figure 4. Typical family of curves $C_p(\lambda)$ for various values of β. Adapted from reference [6].

Figure 4 shows an example of the relationship $C_p(\lambda)$, for different values of β. Paying close attention to this figure, it can be seen that the maximum value of C_p is close to 0.4 and not to 0.593, as predicted by the *Betz limit*. This difference is due to the parameters that were not taken into account when the *Betz limit* was calculated, such as shape and interference of blades.

http://dx.doi.org/10.5772/63432

In addition, that figure also shows that for each value of β there is a value of λ that maximises C_p. It is important to understand this fact because MPCCs will be always defined in order to optimise the SWT electrical generation (working with the maximum value of C_p).

Other point to consider might be the influence of the SWT type on the relationship C_p (**Figure 5**). This figure allows us to identify the families of turbines that produce a higher value of C_p and consequently a higher efficiency. These families are one-bladed, two-bladed and three-bladed. That is the reason why the worldwide major manufacturers usually produce those types of turbines.

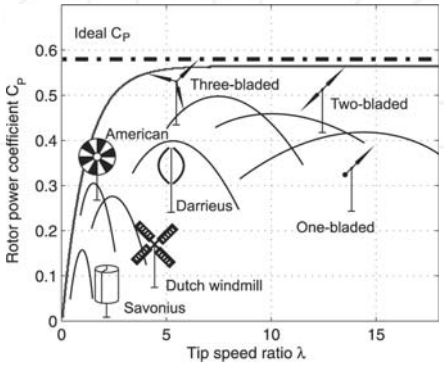

Figure 5. Typical family of curves $C_p(\lambda)$ for different SWT types.

Having explained all this, a simple study of forces occurring in SWT blades will be developed. In **Figure 6**, you can see that when the wind u_h hits a blade, a component u_g appears due to the displacement or blade rotation. The addition of these two components will result in the vector c.

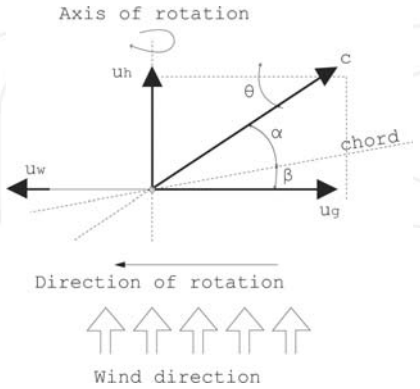

Figure 6. Velocities acting on a blade of a horizontal SWT.

On one hand, the wind component u_h will allow us to calculate the forces that arise on the blade at the turbine input. On the other hand, component c will allow us to do the same, but in this case, at the turbine output. Moreover, three angles will be defined: angle between the blade chord and c, called *attack angle* (α), angle between the rotation plane and c (θ) and angle between the blade chord and the rotation plane, called *pitch angle* (β).

The resultant force F (in its aerodynamic centre) will be used to calculate the SWT speed. That force will be obtained either with the SWT input wind u_h or with the SWT output wind c:

- Forces at the SWT input: In this case, the wind, which hits the blade at the input u_h, produces two kinds of forces: one in the direction of rotation axis F_{axial} and another in the perpendicular direction. This last one causes the SWT rotation F_{torque}. Adding F_{axial} and F_{torque}, the resultant force F will be obtained (**Figure 7**).
- Forces at the SWT output: In the other case, if the vector F is decomposed according to the direction of the apparent velocity c and its perpendicular, the drag force F_{drag} and the lift force F_{lift} will be obtained. The latter two forces are usually associated in a parameter, called L/D, where L is the lift force F_{lift} and D is the drag force F_{drag} (**Figure 7**).

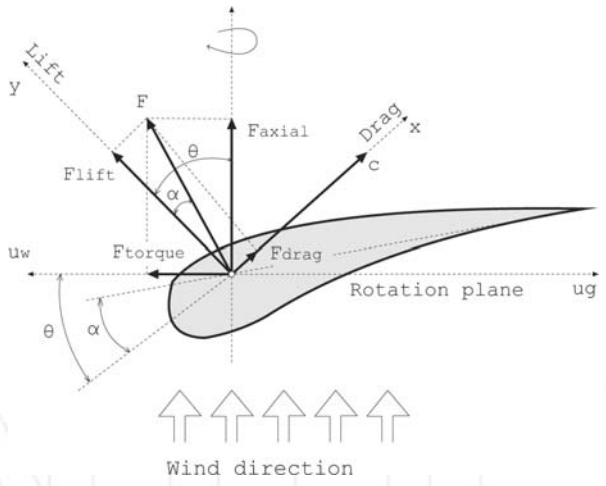

Figure 7. Forces acting on a blade of a horizontal SWT.

This parameter gives an idea of whether the blades are well designed or not. On one hand, the lower the value of L/D is, the greater the influence of F_{drag} will be and the lower the blade speed u_w will be. And on the other hand, the higher the value of L/D is, the greater the influence of F_{lift} will be and the higher the blade speed u_w will be.

Eq. (14) allows us to calculate an initial value of C_p. This relation assumes that C_p depends on λ, L/D and N (number of SWT blades). This equation is known as correlation of Wilson (1976) worldwide [8].

http://dx.doi.org/10.5772/63432

$$C_p = \frac{16}{27}\frac{\lambda}{\lambda + \frac{1.32 + \left(\frac{\lambda - 8}{20}\right)^2}{N^{2/3}}} - 0.57\frac{\lambda^2}{\frac{L}{D}\left(\lambda + \frac{1}{2N}\right)} \tag{14}$$

Although Eq. (14) is an expression that does not take into account many parameters, it will help us to achieve an initial power coefficient C_p. Once C_p is calculated, it will have to be reduced by means of a percentage. This reduction will help us to get a value of C_p which takes into account the rest of the parameters that were initially ignored. Thus, a value closer to the real one can be obtained.

Figure 8 shows an example obtained using Eq. (14), assuming $N = 3$. In the figure, it can be clearly seen, as it had been previously deduced from the study of wind forces, that higher values of L/D produce higher power coefficients C_p and therefore, higher mechanical powers P_w.

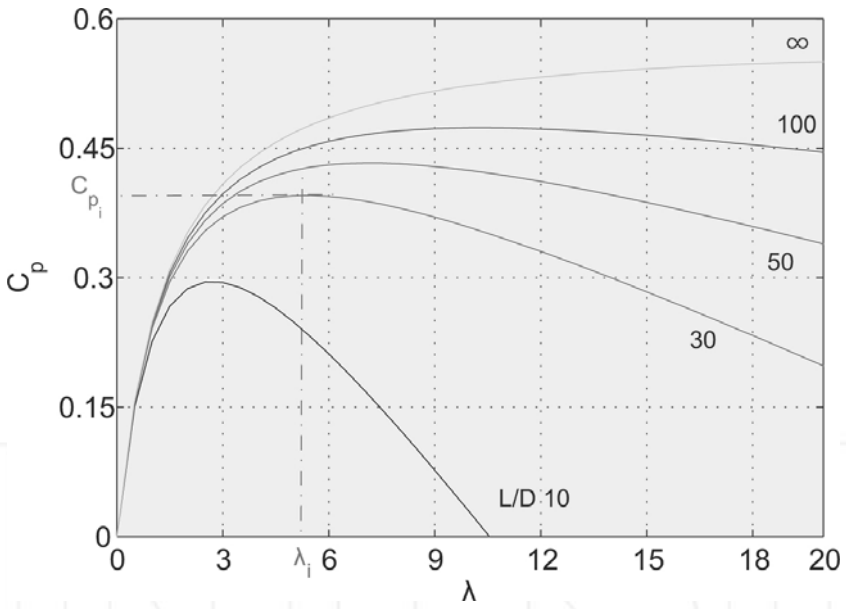

Figure 8. Example of C_p vs. λ for several values of L/D.

During the design of the SWT blades, you will have to make sure that the combination of the parameters λ and L/D produces a maximum value of C_p. That is the reason why a constant relation L/D along the entire blade is searched for. Therefore, it is easy to understand that each SWT will have its own relation L/D.

Eq. (11) and (14) yield the following relation:

$$P_w = \left(\frac{1}{2}\frac{\pi d^2}{4}\rho u_1^3\right)\left(\frac{16}{27}\frac{\lambda}{\lambda + \frac{1.32 + \left(\frac{\lambda - 8}{20}\right)^2}{N^{2/3}}} - 0.57\frac{\lambda^2}{\frac{L}{D}\left(\lambda + \frac{1}{2N}\right)}\right) \tag{15}$$

Using Eq. (15), the value of P_w can be obtained, for

- Constant values of N, d, ρ and L/D.
- Different values of n and u_h, where u_h is obtained from Eq. (6), and n is the SWT rotation speed (rpm) and can be obtained as,

$$n[rpm] = \omega\left[\frac{rad}{s}\right]\cdot\frac{60}{2\pi} \tag{16}$$

In the example of **Figure 9**, the relationship $P_w(n)$, for various wind speeds u_h, can be seen. Paying close attention to this figure and assuming a constant wind speed u_h, two conclusions can be drawn: (1) When the SWT rotation speed n increases, the mechanical power in the shaft P_w also does it and (2) P_w increases up to a maximum value from which it decreases.

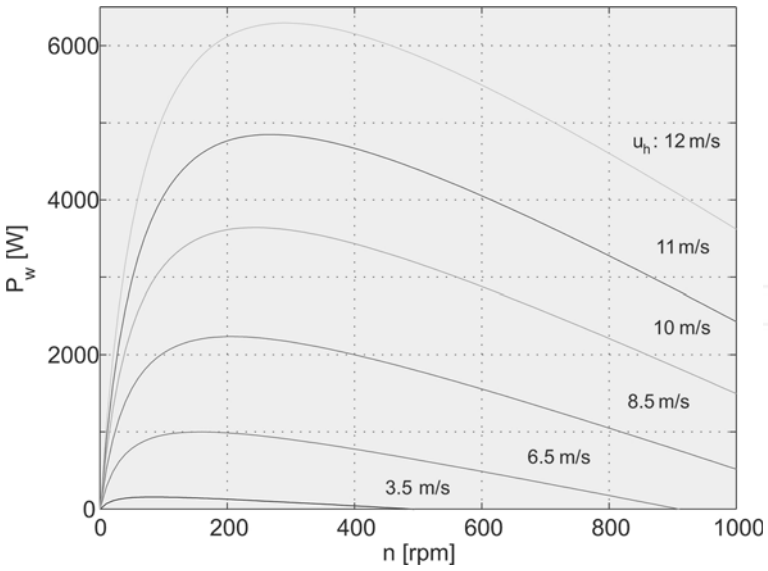

Figure 9. P_w vs. n for various wind speeds u_h and assuming $L/D = 30$.

http://dx.doi.org/10.5772/63432

Having explained this, it is easy to understand that if any change was introduced in the SWT, it should be studied whether this modification varies the value of λ or not. Analysing **Figure 8** and assuming $L/D = 30$, you can observe that for a value of $\lambda = \lambda_i$, the corresponding value C_{pi} is maximum. Thus, if some parameters of which are mentioned above are modified, it is very likely that the value of λ also varies, by moving either left or right. Therefore, the increase or decrease in λ causes a reduction in the power coefficient C_p and with it a drop in mechanical power P_w.

SWTs are designed in order to maximise the value of C_p. In this way, if any change is introduced into the system, it is important to verify that the tip-speed ratio λ remains constant. For this reason, all MPCCs that will be entered in the inverter are calculated in order to ensure a specific constant value of λ_i.

To get this value of λ_i, it is required that for all wind speeds u_{hi}, the SWT turns at a specific speed n_i. In other words, to get a maximum mechanical power P_{wi}, it will be necessary that

- The value of λ_i is constant.
- The value of λ_i provides the maximum power coefficient C_{pi} (**Figure 8**).

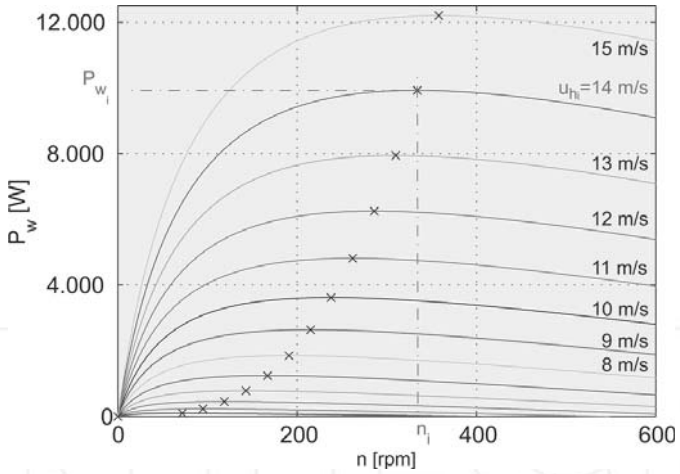

Figure 10. Maximum power point tracker (MPPT), assuming $L/D = 30$. P_w vs. n for several values of u_h.

The example of **Figure 10** shows the maximums of P_w for every wind speed u_h (highlighted points). Therefore, if a maximum mechanical power P_{wi} wants to be obtained for a specific wind speed u_{hi}, it will be necessary to turn the SWT to a particular rotation speed n_i.

If all these maximums are plotted in a new curve, the relationship $P_{w,max}(n)$ is obtained (**Figure 11**). This curve is known as the maximum power point tracker (MPPT).

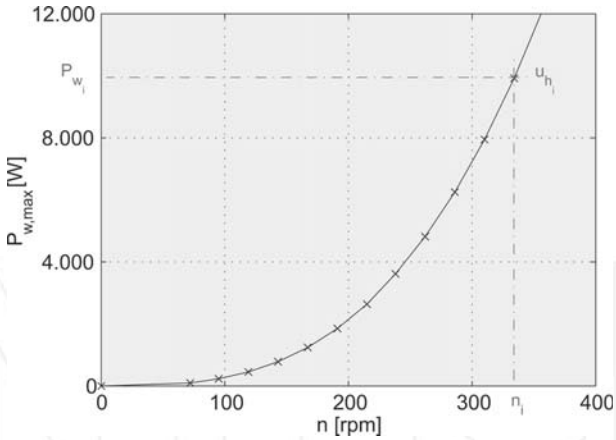

Figure 11. Maximum power point tracker (MPPT), assuming $L/D = 30$. Curve created with the maximums of P_w.

Figure 11 has the special characteristic that all its points provide a maximum value of P_w and consequently a maximum value of C_p. That is the reason why all the points have associated a constant value of λ.

Moreover, considering Eq. (17), which relates mechanical power P_w with torque T_w and with rotation speed ω, the optimal relationship between T_w and n can be also obtained. It will be known as maximum torque point tracker (MTPT; see e.g. in **Figure 12**):

$$P_w = T_w \omega \tag{17}$$

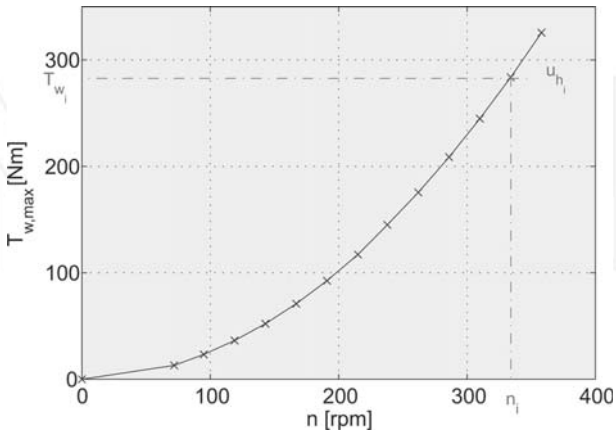

Figure 12. Maximum torque point tracker (MTPT), assuming $L/D = 30$.

http://dx.doi.org/10.5772/63432

2.3. Capacitor banks in an SWT

As it is known, if the electrical machine is working in the no-load test, it provides a rated voltage v_o at the output of the machine. Then, if an electrical load is connected to the machine output, the voltage v_o is reduced. This reduction is due to the emergence of a current in the armature winding that generates a voltage drop in that winding. Moreover, it also produces a magnetomotive force, which reacts with the magnetomotive force generated by the inductor. In this way, the air-gap magnetic flux is modified [5].

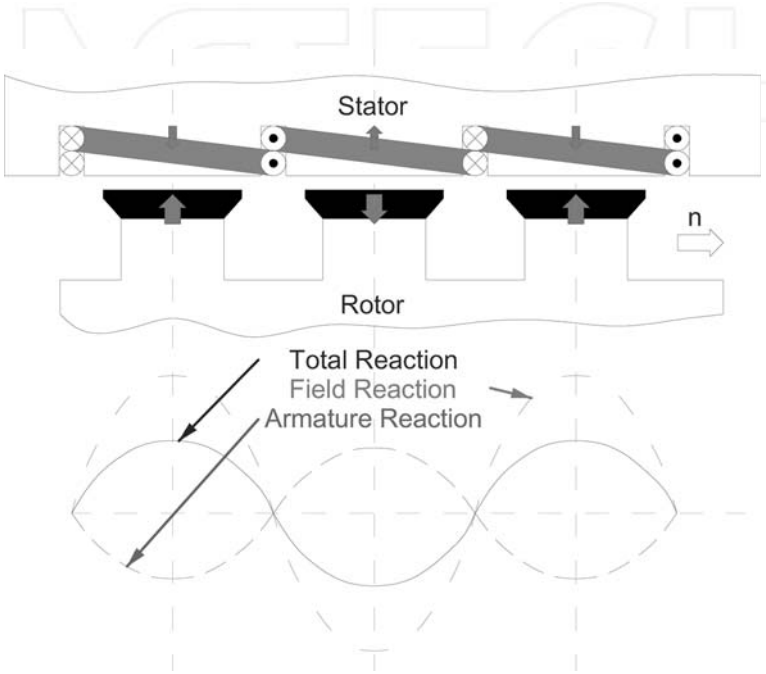

Figure 13. Magnetic field behaviour inside an electrical generator, connecting an inductive load.

Depending on the type of load that is connected to the output of the electrical machine, this effect may vary. On one hand, if an inductive load is connected to the electrical machine output, then the magnetomotive force caused by the armature reaction goes against the magnetomotive force caused by the inductor. This effect is known as the demagnetising effect (**Figure 13**).

On the other hand, if a capacitive load is connected to the electrical machine output, the opposite happens. The magnetomotive force caused by the armature reaction is additive to the magnetomotive force caused by the inductor. This effect is known as the magnetising effect (**Figure 14**).

Thus, an increase in the electrical machine magnetic field can be obtained by connecting a capacitor bank to the electrical machine output.

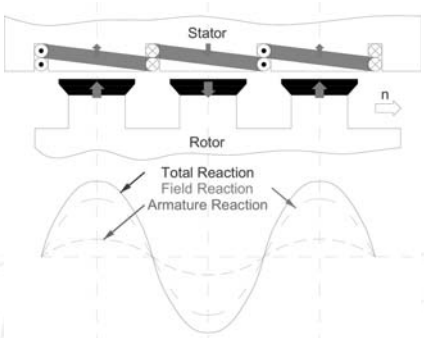

Figure 14. Magnetic field behaviour inside an electrical generator, connecting a capacity load.

2.4. Methodology for calculation of the optimal capacitor bank and the MPCCs

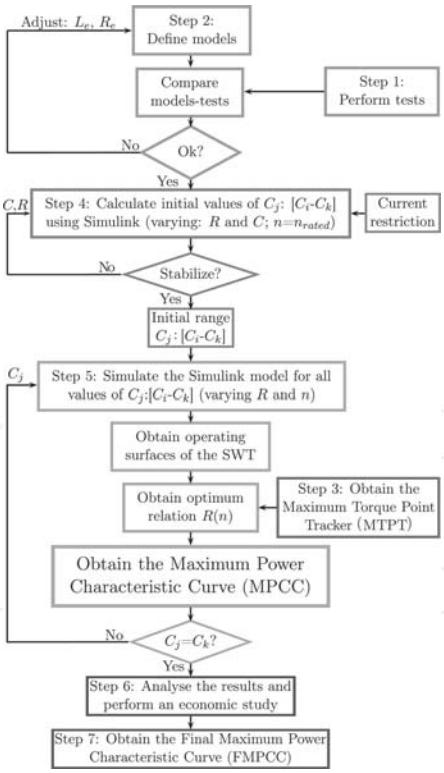

Figure 15. Flowchart of the methodology.

http://dx.doi.org/10.5772/63432

Figure 15 presents the flowchart for calculating the optimal capacitor bank and associated MPCC. The steps of the methodology are as follows:

Step 1: Perform several tests on the real SWT. At a minimum, a no-load test and a rated load test should be carried out.

Step 2: Define a system model.

A system model is needed in order to use the methodology presented here (i.e. using Matlab Simulink or using Finite Element Methods). Such a model makes it possible to analyse the SWT in detail and to evaluate its performance under various operating conditions.

The different parts of the SWT model are electrical machine, rectifier, grid power control (inverter and grid) and capacitor bank (**Figure 16**).

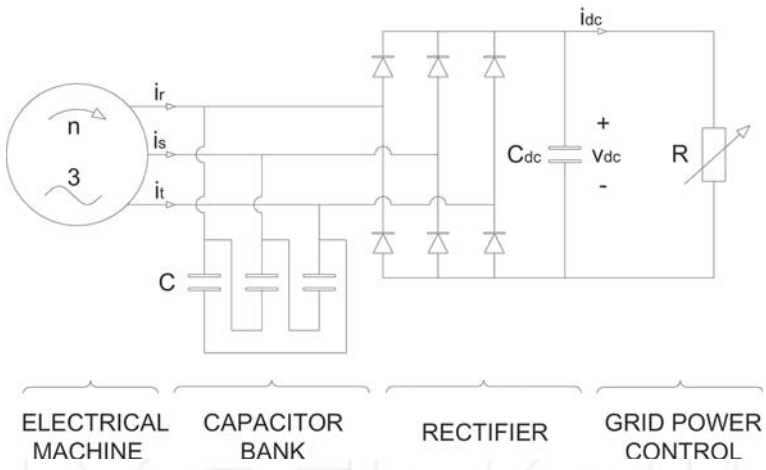

Figure 16. Wind power generation system.

Adjust model parameters by comparing simulation results with those obtained in Step 1. Thus, a reliable model of the system can be defined (**Figure 16**).

Step 3: Calculate the MTPT to extract the maximum power of the wind.

Using the SWT-rated parameters and Eq. (11) and (17), the optimal relationships $P_w(n)$ and $T_w(n)$ can be obtained (**Figures 11** and **12**).

Note that the MTPT must remain unchanged for every value of the variable resistor R. Therefore, MTPT in 3D can be represented as a parallel surface to axis R (**Figure 17**).

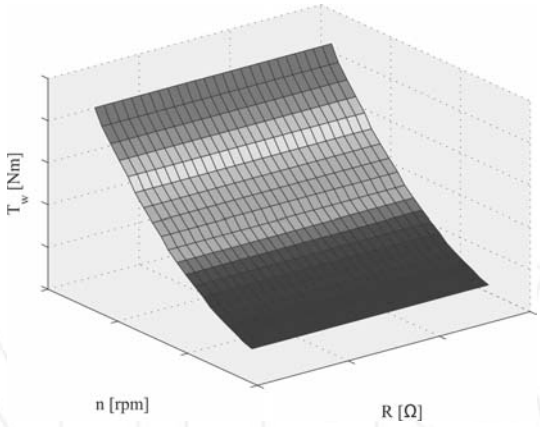

Figure 17. MTPT in 3D.

Step 4: Calculate a capacity range [C_i–C_k], which contains the optimal capacitor *C*.

In order to find this range, a simulation will be performed varying *R* and *C* for the SWT-rated speed. The initial ranges of *R* and *C* must be wide enough to effectively analyse the SWT performance.

Figure 18 indicates that by increasing the capacity *C* for each value of *R*, the power injected into the grid P_{grid} increases up to a maximum capacity C_{max}, from which point P_{grid} decreases. Thus, the value of C_{max} that maximises the P_{grid} is obtained.

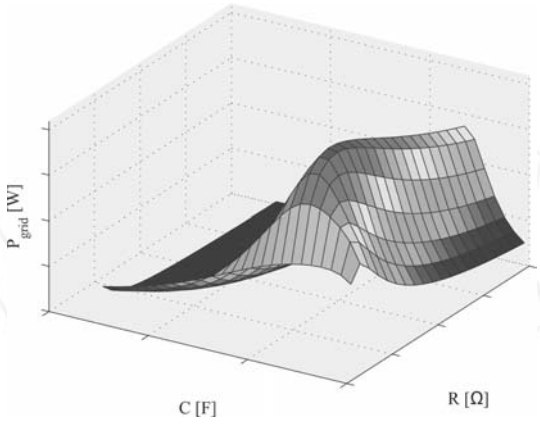

Figure 18. Grid power P_{grid} vs. resistor *R* and capacity *C* for the rated speed n_r.

However, the value of C_{max} must be controlled because it could also increase the current $i_{r,s,t}$ flowing into the electrical machine windings and thereby cause damage (**Figure 16**). Therefore,

http://dx.doi.org/10.5772/63432

it is important to know the winding wire diameter to determine the maximum current $i_{r,s,t,max}$ that can flow through the windings.

Once the value of $i_{r,s,t,max}$ is known, the capacity range [C_i–C_k] can be obtained by means of drawing a perpendicular surface to the axis $i_{r,s,t}$ (see an example in **Figure 19**).

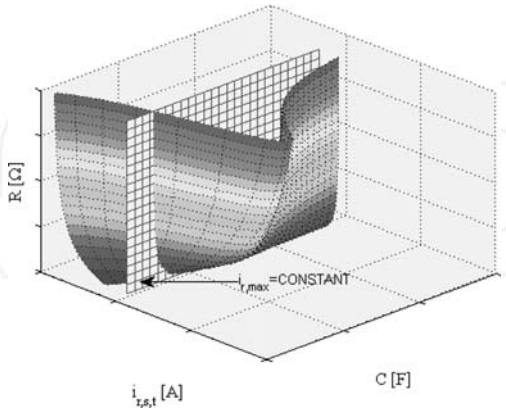

Figure 19. Relationship $R(C)$ not exceeding the restriction of $i_{r,s,t,max}$ and for the SWT-rated speed. Winding current $i_{r,s,t}$ vs. resistor R and capacity C.

By representing the intersection of both surfaces on the plane C–R (**Figure 20**), the capacity values that might be connected, for different values of the resistor R, can be determined. In this way, the current value that could damage the electrical machine will not be reached. So, the capacity range [C_i–C_k] is determined.

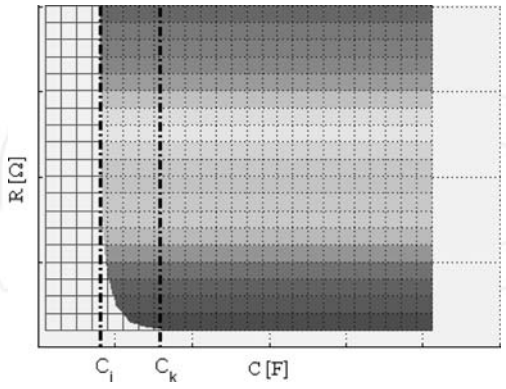

Figure 20. Relationship $R(C)$ not exceeding the restriction of $i_{r,s,t,max}$ and for the SWT-rated speed. Capacity C vs. variable resistor R.

Step 5: Obtain MPCCs for several values of C.

Perform simulations, varying n and R, for constant values of C within the range $[C_i–C_k]$. It should be borne in mind that the more the values of C you test, the more accurate the results will be. For each value of C, the following steps need to be performed:

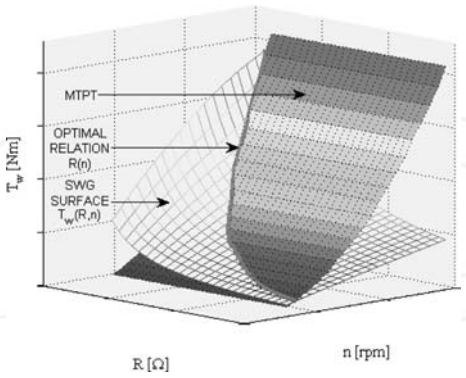

Figure 21. 3D Intersection between the MTPT and the SWT operating surface $T_w(R,n)$.

- **Step 5.1**: Use the system model to determine the SWT operating surface $T_w(R,n)$. Then, obtain the intersection of that surface with the MTPT (**Figure 21**). Thus, the relationship $R(n)$ for maximum mechanical power extraction from wind is given (**Figure 22**).
- **Step 5.2**: Project the optimal relationship $R(n)$ perpendicular to the R-n plane (**Figure 23**).
- **Step 5.3**: Use the model to determine the SWT operating surfaces $P_{grid}(R,n)$ (**Figure 23**) and $v_{dc}(R,n)$ (**Figure 24**). After that, derive the intersection of those SWT surfaces with the surface obtained in Step 5.2. In this way, the optimal relationships $P_{grid}(n)$ and $v_{dc}(n)$ will be determined.

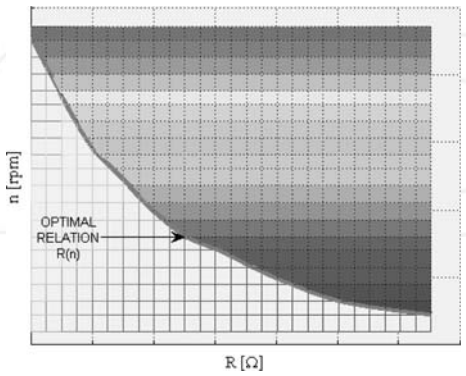

Figure 22. Intersection between the MTPT and the SWT operating surface $T_w(R,n)$. Optimal relationship $R(n)$.

http://dx.doi.org/10.5772/63432

- **Step 5.4**: Finally, combining the values of $P_{grid}(n)$ and $v_{dc}(n)$, the optimal relationship $P_{grid}(v_{dc})$, also known as the MPCC, can be easily determined (**Figure 25**).

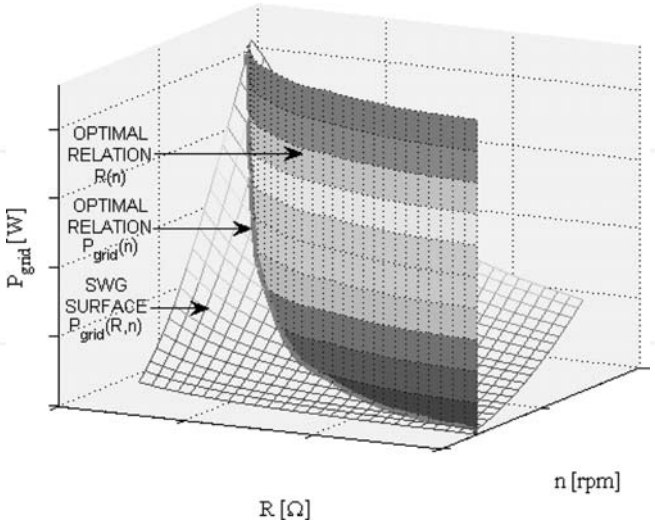

Figure 23. Three-dimensional intersection between the optimal relationship $R(n)$ and the SWT operating surface $P_{grid}(R,n)$.

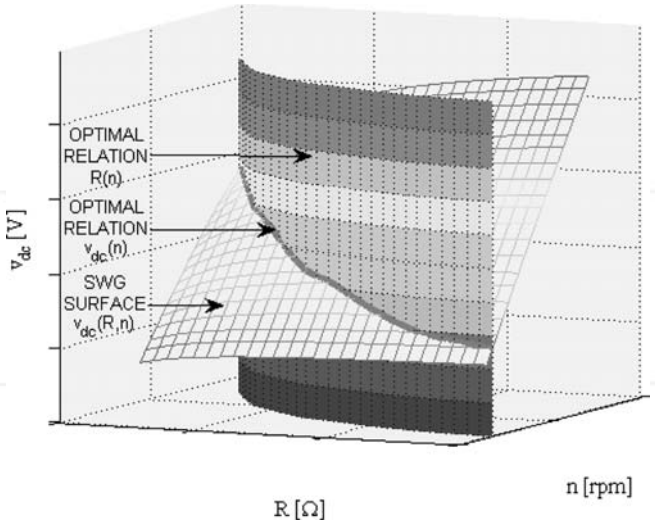

Figure 24. Three-dimensional intersection between the optimal relationship $R(n)$ and the SWT operating surface $v_{dc}(R,n)$.

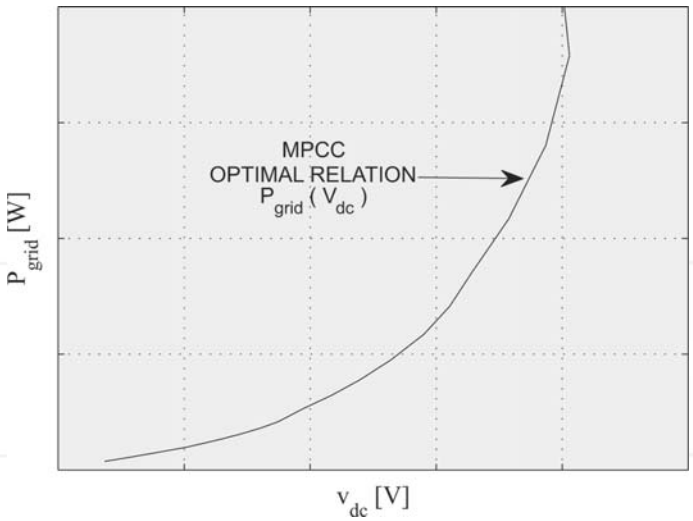

Figure 25. Maximum power characteristic curve (MPCC): grid power P_{grid} vs. rectifier DC voltage v_{dc}.

By repeating Steps 5.1 to 5.4 for each value of *C*, the additional MPCCs can be obtained.

Step 6: Analyse the results and perform an economic study.

To perform the analysis, the well-known Weibull distribution (WD) will be used [3, 9, 10]. This distribution is defined as:

$$W(u_h) = \frac{K}{u_h}\left(\frac{u_h}{u_m}\right)^K e^{-\left(\frac{u_h}{u_m}\right)^K} \tag{18}$$

where K is the shape parameter of the WD, and u_m is the average wind speed.

Wind Class	u_m (10 m)	u_m (50 m)
1	0–4.4	0–5.6
2	4.4–5.1	5.6–6.4
3	5.1–5.6	6.4–7
4	5.6–6	7–7.5
5	6–6.4	7.5–8
6	6.4–7	7–8.8
7	7–9.4	8.8–11.9

Table 1. Wind classification according to average speed. Adapted from reference [11].

http://dx.doi.org/10.5772/63432

Nevertheless, if this distribution is going to be used, certain features of the location where the SWT will be placed need to be known. The National Renewable Energy Laboratory (NREL) defines seven different wind classes (WC). The WC is a function of the average wind speed u_m and the height at which the SWT will be located with respect to the ground (10 or 50 m) [11]. These WCs can be seen in **Table 1**.

Figure 26 represents the WD (Eq. 18) for a value of $K = 1.9$ and for average wind speeds listed in **Table 1** (assuming a height of 10 m).

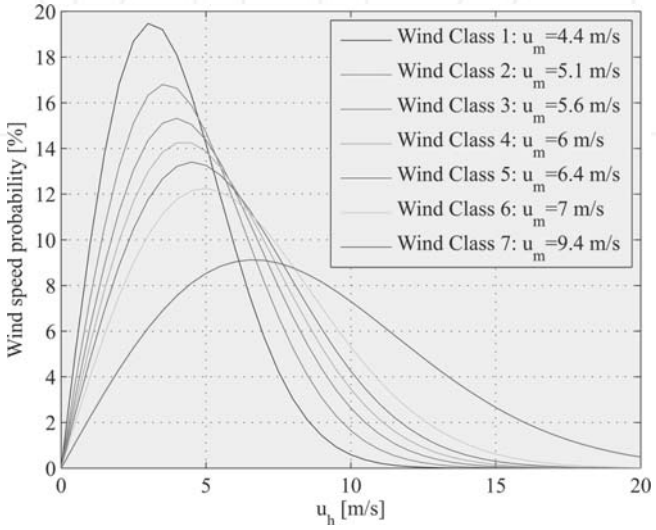

Figure 26. Weibull distribution for different WCs and a height of 10 m.

To compare the results obtained with different values of C, four parameters may be used: $P_d(u_h)$, E_{tot}, $\Delta\eta$ and $\Delta€$.

- $P_d(u_h)$ is the SWT power density and is defined as:

$$P_d(u_h) = W(u_h)\frac{P_{grid}(u_h)}{P_{rated}} \tag{19}$$

where P_{grid} (u_h) is the grid power for each wind speed u_h, and P_{rated} is the rated power of the SWT.

- E_{tot} is the annual total energy that can be produced by the SWT. It is obtained from the following equation:

$$E_{\text{tot}} = 8760\left[\frac{hours}{year}\right]\sum\left(W(u_h)P_{grid}(u_h)\right) \tag{20}$$

- $\Delta\eta$ represents the increment in annual total energy injected into the grid (E_{tot}) for different capacitor banks ($C = C_j$), as compared to the case without a capacitor bank ($C = 0$).

$$\Delta\eta = \frac{E_{tot,C=C_j} - E_{tot,C=0}}{E_{tot,C=0}} \tag{21}$$

$\Delta€$ represents the annual financial benefit obtained by using different capacitor banks ($C = C_j$), as compared to the case without a capacitor bank (C = 0).

$$\Delta€ = \left(E_{tot,C=C_j} - E_{tot,C=0}\right).Energycost\left[\frac{€}{kWh}\right] \tag{22}$$

Step 7: Obtain the final maximum power characteristic curve (FMPCC).

To determine the FMPCC, it is necessary to calculate, for each wind speed u_h, the capacity C that supplies the maximum grid power P_{grid}. Thus, the optimal relationship $C(u_h)$ is calculated. The FMPCC will be made up of sections of the MPCCs that were obtained for different values of C.

3. Conclusions

The increasing development of small-wind energy has made it necessary to study new methods that improve their efficiency. This chapter presents a methodology to increase the SWT efficiency by using a capacitor bank. This methodology will use an electrical model to simulate the system.

It has been shown that connecting different capacitor banks to the system modifies SWT performance and the MPCC. The power obtained from the SWT increases as a result of connecting capacitor banks and is only limited by the maximum current that can flow through the electrical machine windings.

It must be taken into account that it is necessary to know the location of the SWT and the associated average wind speed in order to connect the optimal capacitor bank.

The methodology described in this work could be used by electrical machine manufacturers to optimise the efficiency of SWTs [12] or to reduce the generator size because a new electrical machine with a capacitor bank would include the following modifications in order to obtain the same power: less copper (the capacitor bank decreases the current that flows through the electrical machine), smaller magnet size (magnetising effect of the capacitors) and fewer magnetic plates.

http://dx.doi.org/10.5772/63432

If these modifications are included in SWT design, manufacturing costs would decrease substantially and even more so in the case of higher WCs.

Nomenclature

a:	Induced axial velocity coefficient.
A:	Area of tube in turbine (m^2).
A_1 & A_2:	Area at inlet and outlet of tube (m^2).
c:	Apparent wind speed (m/s).
C:	Capacitor (F).
d:	Swept diameter of the SWT blades (m).
E_{c1} &E_{c2}:	Kinetic energy at inlet and outlet of tube (J).
E_{tot}:	Annual total energy extracted from SWT (kWh).
F:	Resultant force on SWT blade (N).
F_{axial}:	Axial force on SWT blade (N).
F_{torque}:	Force that causes the turn of SWT blade (N).
F_{drag}:	SWT drag force (N).
F_{lift}:	SWT lift force (N).
$i_{r,s,t}$:	Electrical machine phase current (A).
K:	Shape parameter of the Weibull distribution.
m:	Air mass (kg).
n:	SWT rotation speed (rpm).
N:	Number of SWT blades.
P_d:	SWT power density (kWh).
P_{grid}:	Electrical power injected to the grid (W).
P_{rated}:	SWT-rated power (W).
P_w:	Mechanical power extracted from wind (W).
p_+ &p_-:	Air pressure before and after turbine (Pa).
R:	Variable resistor (Ω).
T_w:	Torque in the shaft of the SWT (Nm).
u:	Wind speed (m/s).
u_1 &u_2:	Wind velocity at inlet and outlet of tube (m/s).
u_a:	Induced axial velocity (m/s).
u_g:	Wind velocity due to rotation of blades (m/s).

u_h: Wind velocity in turbine (m/s).

u_m: Wind average speed of the Weibull distribution (m/s).

v_{dc}: DC voltage (V).

v_o: Rated voltage at the output of the electrical machine (V).

u_w: Linear velocity of SWT blades (m/s).

W: Weibull distribution.

α: Attack angle [°].

β: Pitch angle [°].

θ: Angle between the rotation plane and c [°].

λ: Tip-speed ratio.

ρ: Air density (kg/m^3).

ψ: {SWT orientation angle with respect to air (°).

ω: SWT angular speed (rad/s).

Author details

Alberto Arroyo*, Mario Manana, Pablo B. Castro, Raquel Martinez, Ramon Lecuna and Juan Carcedo

*Address all correspondence to: arroyoa@unican.es

University of Cantabria, Santanderm, Spain

References

[1] Pullen A. and Sawyer S. Annual Market Update 2010. Global Wind Report. Global Wind Energy; 2010, Brussels, Belgium.

[2] Kesraoui M., Korichi N., and Belkadi A. Maximum power point tracker of wind energy conversion system. Renewable Energy. 2011;36:2655–2662.

[3] Milivojevic N., Stamenkovic I., and Schofield N. Power and energy analysis of commercial small wind turbine systems. In: Industrial Technology (ICIT); 2010. p. 1739–1744.

[4] Fuchs E.F., Vandenput A.J., Holl J., and White J.C. Design analysis of capacitor-start, capacitor-run single-phase induction motors. Energy Conversion. 1990;5:327–336.

[5] Umans C., Fitzgerald S., and Kingsley A.E., editors. Electric Machinery. McGraw Hill; 2003, New York.

[6] Rodríguez S., Arnalte J.L., and Burgos J.C., editors. Electric systems of Electric Power Production. Spain: Editorial Rueda S.L.; 2003. 450 p.

[7] Kuik G.A.M., editor. The Lanchester Betz Joukowsky limit. Wind Energy. 2007;10:289-291. DOI: 10.1002/we.218

[8] Wilson R.E. and Lissaman B.S. Aerodynamic Performance of Wind Turbines. Office of Science. U.S. Department of Energy; 1976, United States.

[9] Sathyajith M., editor. Wind Energy. Fundamentals, Resource Analysis and Economics. Springer; 2006. The Netherlands. DOI: 10.1007/3-540-30906-3.

[10] Yu Z. and Tuzuner A. Wind speed modeling and energy production simulation with Weibull sampling. In: Power and Energy Society General Meeting. Conversion and Delivery of Electrical Energy in the 21st Century, IEEE; 2008. p. 1–6.

[11] Elliot D.L., Holladay C.G., Barchet W.R., Foote H.P., and Sandusky W.F., editors. Wind Energy Resource Atlas of the United States. Golden, CO: U.S. Department of Energy Pacific Northwest; 1986.

[12] Arroyo A., Manana M., Gomez C., Fernandez I., Delgado F., and Zobaa A. A methodology for the low-cost optimisation of small wind turbine performance. Applied Energy. 2013;104:1–9. DOI: 10.1016/j.apenergy.2012.10.068

INTECH